

Fault Models for Quantum Mechanical Switching Networks

Jacob D. Biamonte,^{*} Jeff S. Allen and Marek A. Perkowski

Portland State University, Portland, Oregon 97201, USA

Received: August 18th, 2005 / Revised version: date

Key words *Fault Modeling, Reversible Computers, Quantum Computers.*

Abstract This work justifies several quantum gate level fault models and discusses the causal error mechanisms thwarting correct function. A quantum adaptation of the classical test set generation technique known as constructing a fault table is given. This classical technique optimizes test plans to detect all the most common error types. This work therefore considers the set of predominate errors modeled by unwanted qubit rotations. In classical test, a fault table is constructed allowing the comparison between a circuit's nominal response and a response perturbed by each separately considered error. It was found that isolating a correct circuit from a circuit containing any of the Pauli Fault rotations, requires applications of just two independent test vectors. This is related to the proven fact that a reversible system preserves the probability that additional information may be present. Thus, the probability of detection for an observable fault is related only to the probability of presence. A theorem that better connects classical ideas to quantum test set generation is presented. This leads directly to a relationship between the deterministic presence of a fault in the state vector observed with some probability and the probabilistic presence of a fault observed deterministically (Relating Time and Space Error Models).

1 Introduction

The difficulty of extending classical test theory [1][2] has been a subject of discussion [3] in recent times, with the main results reported in [4][5][6][7]. Despite this and recent interest by several other authors, adequate justification has yet to be given for any of the fault models used. Much of the current research has applied the classical stuck at fault model, in which a lead is permanently connected to a power rail or to a ground, directly to quantum circuits. We however, present a comprehensive analysis of gate level errors impacting quantum circuits. The faults justified in this work will lead to the adaptation of classical methods that can address the quantum test problem by considering physically realistic error models.

Experimental physicists who build quantum circuits [8] have not experienced much need to research optimized testing methods due to the current attainable qubit count [9][10][11][12]. All current approaches to the quantum test problem are consequently exhaustive. The main approach now is to use process tomography such that for a system of n qubits 2^n initial states necessitate 2^n measurements, for a complexity of $\Theta(2^{2n})$ and a growth rate proportional to the experimental accuracy desired [13][14]. In a second approach (known as ancillary assisted process tomography [15][16]), n qubits are *mirrored* replacing 2^n initial states with an n dimensional state space entangled with each of the 2^n basis states of the system under test. However, in this approach any reduction in initial states increases measurement complexity, therefore the only offered advantage is experimental simplification (such as in optics [17]). Quantum computers are known to solve classically intractable problems [18][20]. However, the time required to test these circuits using current process validation methods is also intractable.

Classically [19] a test set complete for the stuck fault model, propagates both binary values 0 and 1, quantum mechanically known as basis vectors $|0\rangle$ and $|1\rangle$, through all nodes in a circuit. This allows for all nodes to be completely tested and partially verifies the function of many gates. A major weakness of

* J.B. is the author with whom electronic correspondence shall be addressed: biamonte@ieee.org

this fault model applied to quantum circuits is that it assumes deterministic locality in the state acted on by all gates in the circuit. Furthermore, it is very possible to develop test sets for reversible and quantum circuits complete for the stuck at model, that never turn on a gate [21].

In this work, a quantum circuit is viewed as an abstract structure of gates, mathematically represented as unitary matrices that describe quantum evolution. Quantum circuits are wired together using direct field interactions and gates are built by applying a force. By using properly justified fault models, test patterns that sample the interconnectivity of the network nodes, wires and gates in an attempt to locate maximum structural instability and minimal structural connectivity can be developed. Consequently, this work puts forth several functional fault models defined as Axioms and dependent on the structure of quantum gates comprising a given network. Test plans complete for functional fault models drive the quantum circuit to its bounds of operation determining if any faults are present in the interconnections of the quantum network or internal to gates.

Classically, one may define a testability measure as a product of observability and controllability. An entangled state is hard to control and therefore has decreased controllability and the observability of a fault present in the state generally leads to probabilistic measurement outcomes. The controllability of a circuit represents an ability to propagate a specific input vector through a network, such that it will map a test vector to a place of fault. This represents an added challenge in the case of quantum circuits, since inputs will become entangled and in many cases location specific (local) inputs may not be possible. The classical and quantum degrees of freedom possible in a gate are therefore considered separately. Some of the fault models defined have the same form as the cell fault model [2], with different motivation. Quantum faults are represented as Axioms to avoid the complications experienced with controllability. These Axioms are designed to logically test the gate level function of all network components.

1.0.1 Structure of the paper We begin by first giving a background of quantum mechanics in Sec. 1.1. This is followed by presenting a simple quantum computation in Sec. 1.2. Sec. 2 presents the current state of the art in quantum process validation. Next Sec. 3 discusses the quantum fault models used in this study. The intended audience are engineers and test theorists wishing to extend classical ideas to respective quantum counterparts. A quantum adaptation of the classical test set generation technique known as constructing a fault table is given in Sec. 4. This is followed by the conclusion in Sec. 5.

1.1 Background

In this work, a basic knowledge of quantum circuits is assumed. The field is now well established with adequate background appearing in several texts such as [22]. Most literature however, introduces only the state vector. Due to the importance and wide spread use in error modeling the following introduction of the density operator formalism is given.

In quantum computation, classical bit registers are replaced with collections of qubits described by a corresponding density operator, $\rho = \sum_i p_i |\psi_i\rangle \langle \psi_i|$, where $|\psi_i\rangle$ represents a state vector, and ρ has trace one. When $tr(\rho^2) = 1$ the pure states description is complete and when $tr(\rho^2) < 1$ the mixed state of the system lacks information for complete description. The n dimensional state space of quantum computation is a composite complex vector space formed from an algebraic tensor product ($\rho_0 \otimes \rho_1 \otimes \dots \otimes \rho_n$) of density matrices representing component physical systems, ρ acts on this state space.

A set of measurement operators (*observables*) $\{M_m\}$ acting on the state space of a quantum system must be defined, in which index m references the measurement outcomes [22] and $\sum_m M_m M_m^\dagger = I_m$. Consider for example a collection of measurement operators on a two qubit system:

$$\{M_m\} = \{|00\rangle \langle 00|, |01\rangle \langle 01|, |10\rangle \langle 10|, |11\rangle \langle 11|\}. \quad (1)$$

This collection is complete since their sum is the 4×4 identity matrix,

$$|00\rangle \langle 00| + |01\rangle \langle 01| + |10\rangle \langle 10| + |11\rangle \langle 11| = I_4. \quad (2)$$

If ρ is found in eigenstate m , the resulting joint quantum state of the system will be

$$\rho_m = (M_m \rho M_m^\dagger) / tr(M_m^\dagger M_m \rho). \quad (3)$$

The probability of result m is:

$$p(m) = tr(M_m^\dagger M_m \rho). \quad (4)$$

It is helpful to consider that each real number indexed by m along the diagonal of density matrix ρ corresponds to the probability of measuring a quantum system in the basis state with corresponding

index m .¹ System measurement allows m bits of classical information to be extracted. If one or more of these m bits is different than expected, the quantum switching network contained an error.

A quantum program is represented as the evolution of an ideally closed system, described by a unitary transformation U (a matrix). A program must be decomposed into a product of physically realizable operations (matrices), and each elementary operation can be represented as a gate in a quantum circuit. The qubits in the system are initialized to state ρ , and the system evolves with U , according to $\rho' = U\rho U^\dagger$. During evolution it is possible for a register of qubits to reside in superpositions of classical states. Superposition states may be factored, but only to the level of description that is local with respect to single qubits, such as:

$$\begin{aligned}\rho_s &= \frac{1}{2} |00\rangle \langle 00| + \frac{1}{2} |01\rangle \langle 01| + \frac{1}{2} |10\rangle \langle 10| + \frac{1}{2} |11\rangle \langle 11| \\ &= \left(\frac{|0\rangle \langle 0| + |1\rangle \langle 1|}{\sqrt{2}} \right) \otimes \left(\frac{|0\rangle \langle 0| + |1\rangle \langle 1|}{\sqrt{2}} \right).\end{aligned}\quad (5)$$

Evolution may also lead to entangled states that may not be factored to local descriptions, like this one:

$$\rho_e = \frac{1}{2} (|00\rangle \langle 00| + |11\rangle \langle 00| + |00\rangle \langle 11| + |11\rangle \langle 11|).\quad (6)$$

Regardless of physical separation, action of a witness on an entangled component has a composite impact. Furthermore, for an entangled system, component observation leads to classically impossible information gain regarding the state of the composite system, as consequence of altering all states.

We conclude this section with a comment on notational conventions. Normalization constants are often omitted, as is an introduction to state vectors.² Shorthand notation for some common states must be defined, $|+\rangle = |0\rangle + |1\rangle$, $|-\rangle = |0\rangle - |1\rangle$, $|\pm\rangle = |0\rangle \pm |1\rangle$ and $\psi = |\psi\rangle \langle \psi|$. The general notational conventions and vocabulary terms outlined in the textbook by Nielsen and Chuang [22] are used. An example quantum computation is next given.

1.2 Example Quantum Computation

We now outline the details of a simple quantum computation by considering a two qubit quantum processor. The collection of measurement operators defined for a dual bit system given in Eqn. 2 will be used. A useful unitary operator is the quantum controlled-NOT gate (CN_{ct}),³ such that the top control qubit $|a\rangle$ inverts the target qubit $|b\rangle = \{|0\rangle, |1\rangle\}$ whenever the control qubit is in state $|1\rangle$. The function of this gate is illustrated in several ways, the first is, $|a\rangle \rightarrow |a\rangle, |b\rangle \rightarrow |b\rangle \oplus |a\rangle$ where \oplus represents modulo 2 addition. Apart from classical functionality, quantum gates exhibit a feature known as phase kick-back.⁴ That is, if the input state of the target is an eigenvector of the control gate's operation, the eigenvalue of the target state traverses backwards to the activating state of the control qubit(s), leaving the target unchanged up to a global phase. This may be seen from the CN gate's truth table given in Fig. 3. Phase kickback is a feature unique to quantum circuits. All known quantum algorithms utilize phase kickback in some fashion [22]. The unitary matrix representing the CN gate is given in Eqn. 7.

$$CN_{12} = \begin{pmatrix} 1 & 0 & 0 & 0 \\ 0 & 1 & 0 & 0 \\ 0 & 0 & 0 & 1 \\ 0 & 0 & 1 & 0 \end{pmatrix}\quad (7)$$

The CN gate may also be written in what is known as an outer product representation,

$$CN = 1/2(|00\rangle \langle 00| + |01\rangle \langle 01| + |10\rangle \langle 11| + |11\rangle \langle 10|).\quad (8)$$

Finally, Fig. 1 (a) illustrates the CN gate as a quantum circuit. A second common gate that will be used is known as the Hadamard operator: drawn schematically as \boxed{H} , defined algebraically in Eqn. 9 and

¹ For each indexed diagonal entry $0 \leq m \leq 1$ and their sum is 1.

² State vectors are referenced using Dirac Notation, such as arbitrary example, $|\psi\rangle = \alpha |0\rangle + \beta |1\rangle$ and respective conjugate, $\langle \psi| = \alpha^* \langle 0| + \beta^* \langle 1|$. Lecture notes accompanying [22] are given in [23] and D. Deutsch has an informative online video series linked to in Ref. [24].

³ Harrow and Nielsen [25] have shown that the two qubit quantum CN gate is the most robust quantum gate in the presence of depolarizing noise in terms of an ability to generate entanglement.

⁴ See [26], the 1999 PhD thesis of M. Mosca, *Quantum Computer Algorithms*, for background on using quantum phase for various quantum computational tasks.

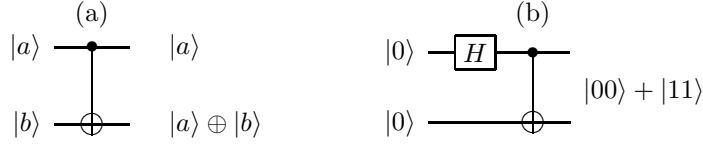


Fig. 1 CN Gate: (a) The action of the CN gate when $|a\rangle$ and $|b\rangle$ are basis state vectors, (b) Using the CN and Hadamard gate to generate an entangled pair.

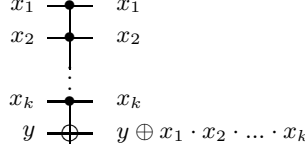


Fig. 2 Arbitrary Quantum k -CN Gate Realizing $y \oplus x_1 \cdot x_2 \cdot \dots \cdot x_k$ on the $(k + 1)^{th}$ qubit.

it's action on some common states are: $|0\rangle \longrightarrow |+\rangle$, $|1\rangle \longrightarrow |-\rangle$, $|+\rangle \longrightarrow |0\rangle$ and $|-\rangle \longrightarrow |1\rangle$.

$$H = \frac{1}{\sqrt{2}}(|0\rangle + |1\rangle)\langle 0| + \frac{1}{\sqrt{2}}(|0\rangle - |1\rangle)\langle 1| \quad (9)$$

With the quantum processor initialized to state $\rho = |00\rangle\langle 00|$, analysis of the quantum circuit depicted in Fig. 1 (b) will be conducted. The first register is acted on with a Hadamard operator,

$$\rho' = (H \otimes I) |00\rangle\langle 00| (H \otimes I)^\dagger = \quad (10)$$

$$\left(\frac{|0\rangle + |1\rangle}{\sqrt{2}} \right) |0\rangle \left(\frac{\langle 0| + \langle 1|}{\sqrt{2}} \right) \langle 0| = \quad (11)$$

$$\frac{1}{2} (|00\rangle\langle 00| + |00\rangle\langle 10| + |10\rangle\langle 00| + |10\rangle\langle 10|). \quad (12)$$

The next operation performed is the CN_{12} gate, with the control and target being the first and the second qubits respectively. The resulting state of the system is now

$$\rho'' = \frac{1}{2} (|00\rangle\langle 00| + |00\rangle\langle 11| + |11\rangle\langle 00| + |11\rangle\langle 11|). \quad (13)$$

Considering the normalization constant the state of the system written as an explicit density matrix is shown in Eqn. 14.

$$\rho = \frac{1}{2} (|00\rangle + |11\rangle)(\langle 00| + \langle 11|) = \frac{1}{2} \begin{pmatrix} 1 & 0 & 0 & 1 \\ 0 & 0 & 0 & 0 \\ 0 & 0 & 0 & 0 \\ 1 & 0 & 0 & 1 \end{pmatrix} \quad (14)$$

Eqn. 4 gives the probability $p(m)$ that the system will be found to reside in a particular state m . This is calculated by using the collection of measurement operators defined in Eqn. 2. For example, given the measurement operator $|00\rangle\langle 00|$, determining the probability that the system will be found in the basis state with corresponding index is $tr(|00\rangle\langle 00| \rho) = \frac{1}{2}$. This means that half of the time the quantum system will be found in the same state as initially prepared, and half the time the quantum system will not be found in that state. The interesting property of the post measurement state and entangled states in general is that— independent of spacial separation—by a single measurement of one qubit, information is gained regarding the state of the second. For a maximally entangled state—such as this example—the state of the second qubit is instantly known by observation of only the first.

Quantum CN gates can have any number of controls. These gates are known as k -CN gates as shown in Fig. 2. They may be implemented via a unitary approximation [22] or by using controlled n^{th} root of NOT gates in the design considered by Barenco et al., (see [27], page 17, § 7; as well as Sec. 3.4). The fault models presented in this work are for general k -CN gates.

This section concludes by providing references to additional quantum computing and quantum physics resources [22][23][24]. In the next section (2) a discussion of the current methods used to test quantum circuits is given.

2 Current Methods Used to Test Quantum Circuits

In the mid to late 90's experimentalists developed a method of black box characterization known as quantum process tomography [14]. A quantum process is described as a map between input and output quantum states, e.g. $\rho_{out} = \mathcal{E}(\rho_{in}) = \sum_j E_j \rho_{in} E_j^\dagger$, where the map \mathcal{E} is a *quantum operation*⁵ and the operators E_j are called operation elements.⁶ Process tomography is a procedure that allows the reconstruction of the behavior of a quantum network by performing state tomography on a set of initial states ρ_i that form an operator basis for the system in question [13].⁷ The input states and measurement projectors in process tomography each form a basis for the set of n -qubit density matrices requiring $d^2 = 2^{2n}$ elements in each set [22], where d is the dimensions of the Hilbert space. For a two-qubit gate $d^2 = 16$, resulting in 256 different settings of input states and measurement projectors. One of many possible input combinations (adapted from the optics experiment in [28]) forming an operator basis needed to characterize the space of two-qubit circuits is the following:⁸

$$\begin{aligned} \{ & |00\rangle, |01\rangle, |10\rangle, |11\rangle, |0+\rangle, |0y-\rangle, |1y-\rangle, |1+\rangle, \\ & |++\rangle, |y_+y-\rangle, |y_++\rangle, |y_++\rangle, |1+\rangle, \\ & |y_+1\rangle, |1+0\rangle, |y_+0\rangle \}. \end{aligned} \quad (15)$$

Of course there exist many possible choices for such a basis. In general however, for a system of n qubits the computational basis states $|0\rangle, \dots, |2^n - 1\rangle$ and superpositions $(|q\rangle \pm |r\rangle)/\sqrt{2}$ are prepared, where $q \neq r$ [32].

Given many copies of an experimental sample, state tomography is a procedure allowing one to reconstruct an arbitrary quantum state to a given accuracy. It requires a set of simple measurement operators that are products of Pauli matrices,

$$\sigma_x = \begin{pmatrix} 0 & 1 \\ 1 & 0 \end{pmatrix} = |1\rangle\langle 0| + |0\rangle\langle 1| \quad (16)$$

$$\sigma_y = \begin{pmatrix} 0 & -i \\ i & 0 \end{pmatrix} = i|0\rangle\langle 1| - i|1\rangle\langle 0| \quad (17)$$

$$\sigma_z = \begin{pmatrix} 1 & 0 \\ 0 & -1 \end{pmatrix} = |0\rangle\langle 0| - |1\rangle\langle 1|, \quad (18)$$

and the identity matrix, $\sigma_i = |0\rangle\langle 0| + |1\rangle\langle 1|$. The method relies on creating a set of orthogonal measurements and using the Hilbert-Schmidt inner product [22] to expand the state of ρ based on the average outcome of each measurement. A single qubit may be reconstructed as the following density matrix:

$$\rho = \frac{tr(\rho)\sigma_i + tr(\sigma_x\rho)\sigma_x + tr(\sigma_y\rho)\sigma_y + tr(\sigma_z\rho)\sigma_z}{2}. \quad (19)$$

Expressions like $tr(\sigma_x\rho)$ in Eqn. 19 refer to an average measurement outcome where σ_x is an observable. A similar expansion to that of Eqn. 19 applies to n bit systems. For example, reconstruction of any two-qubit operator requires a total of $2^{2n} = 16$ measurement observables:

$$\begin{aligned} \{ & \sigma_i \otimes \sigma_i, \sigma_i \otimes \sigma_x, \sigma_i \otimes \sigma_y, \sigma_i \otimes \sigma_z, \sigma_x \otimes \sigma_i, \sigma_x \otimes \sigma_x, \sigma_x \otimes \sigma_y, \sigma_x \otimes \sigma_z, \sigma_y \otimes \sigma_i, \sigma_y \otimes \sigma_x, \\ & \sigma_y \otimes \sigma_y, \sigma_y \otimes \sigma_z, \sigma_z \otimes \sigma_i, \sigma_z \otimes \sigma_x, \sigma_z \otimes \sigma_y, \sigma_z \otimes \sigma_z \}. \end{aligned} \quad (20)$$

A difficulty associated with quantum process tomography is that in experimental practice, the observables are not so easily realized, as they are defined in our purely mathematical model. It turns out that a system with d dimensions requires $16^d - 4^d$ independent parameters to uniquely describe the process [13], where $d = 2^n$. Little growth in the number of qubits possible in the quantum circuits designed today will quickly take memory requirements past current Quantum Automatic Test Equipment (QATE) abilities. The useful method of quantum process tomography was developed out of a need for black box characterization (for that purpose its use appears unavoidable). However, process tomography

⁵ In this work we only consider the case where $\sum_j E_j E_j^\dagger = I$.

⁶ A review of the properties of operation elements is given in Ch. 3 of the 1998 PhD Thesis by Nielsen [29].

⁷ A purely mathematical discussion of process tomography is presented, all measurements are treated as yielding exact probabilities and all sources of error in those measurements are ignored. For experimental background see for example [28] and [30][31]. Chapter 8 in Ref. [22] also has an introduction to both State and Process Tomography.

⁸ Using the notation that: $(|y_+\rangle = |0\rangle + i|1\rangle)$ and $(|y_-\rangle = |0\rangle - i|1\rangle)$. The measurement projectors corresponding to this set of initial states adapted from the optics experiment given in [28] are: $\langle 00|, \langle 10|, \langle +1|, \langle y_-0|, \langle y_-1|, \langle 11|, \langle 01|, \langle 0-|, \langle 0y_-|, \langle y_-y_-|, \langle y_- -|, \langle +-, \langle +y_+|, \langle 1-|, \langle 1y_-|$ and $\langle +0|$.

works independently of the set of gates realized in the network and their possible faults and when used as a method to test quantum switching networks, it has a classical counterpart known as *brute-force* or complete *functional-testing*.

In order to continue discussion, distance measures between quantum states must be introduced. Let us first define the well known Fidelity measure between quantum states.

Definition 1 The **Fidelity** between density matrices ρ and σ is defined as:

$$F(\rho, \sigma) \equiv \text{tr} \left(\sqrt{\sqrt{\rho}\sigma\sqrt{\rho}} \right)^2 \quad (21)$$

When $\rho = |\psi\rangle\langle\psi|$ is a pure state the fidelity has an easy interpretation as the overlap between ρ and σ , reducing to:

$$F(\psi, \sigma) = \langle\psi|\sigma|\psi\rangle. \quad (22)$$

Furthermore, the Fidelity evaluates to zero when pure states are orthogonal, it evaluates to one when identical, and is not considered a metric.⁹ For a discussion regarding an operational interpretation of the Fidelity for a mixed state see Reference [33].

A second common distance measure that will now be defined is known as the Trace Distance between quantum states.

Definition 2 The **Trace Distance** between density matrices ρ and σ is defined as:

$$D(\rho, \sigma) \equiv \frac{1}{2}\text{tr}|\rho - \sigma| \quad (23)$$

where $|Z| = \sqrt{Z^\dagger Z}$. Since $0 \leq D \leq 1$ the trace distance is a genuine metric on quantum states [34][22] and thus has the following three properties: (i) $D(\rho, \sigma) \geq 0$ with $D(\rho, \sigma) = 0$ iff $\sigma = \rho$, (ii) Symmetry: $D(\rho, \sigma) = D(\sigma, \rho)$, and (iii) the Triangle Inequality: $D(\mathcal{E}(\rho), \mathcal{G}(\rho)) \leq D(\mathcal{E}(\rho), \mathcal{F}(\rho)) + D(\mathcal{F}(\rho), \mathcal{G}(\rho))$. The Trace Distance has an obvious compelling physical interpretation as the statistical measurement distinguishability between quantum states. Furthermore, the Trace Distance has the interesting property of contractivity, that is, $D(\mathcal{E}(\rho), \mathcal{E}(\sigma)) \leq D(\rho, \sigma)$ whenever \mathcal{E} is a trace-preserving quantum operation. This just means that acting on arbitrary quantum states ρ and σ both with operation \mathcal{E} will never increase their distinguishability [34][22].

The Trace Distance and Fidelity are complimentary measures and should be considered equally important when comparing two quantum states. Distance measures may also be used to compare and contrast a real process \mathcal{F} and an ideal process \mathcal{E} , such that $\Delta(\mathcal{F}, \mathcal{E})$ defines an error metric on a quantum process [34].

Definition 3 The **S-Fidelity** between real quantum process \mathcal{F} and ideal quantum process \mathcal{E} is defined as:

$$\Delta_{min}^F(\mathcal{F}, \mathcal{E}) \equiv \min_{|\psi\rangle} \Delta(\mathcal{F}(\psi), \mathcal{E}(\psi)) \quad (24)$$

where the minimum is over all possible pure state inputs and Δ is a Fidelity measure on quantum states.

Definition 4 The **S-Distance** between real quantum process \mathcal{F} and ideal quantum process \mathcal{E} is defined as:

$$\Delta_{max}^D(\mathcal{F}, \mathcal{E}) \equiv \max_{|\psi\rangle} \Delta(\mathcal{F}(\psi), \mathcal{E}(\psi)) \quad (25)$$

where the maximum is over all possible pure state inputs and Δ is a Distance metric on quantum states.

Instead of considering all pure states, we will restrict our thinking to a set of inputs needed to form a complete operator basis for the system in question. In this case, experimentally determining the S-Distance/S-Fidelity amounts to performing state tomography on this complete operator basis input set while keeping track of the worst Trace Distance (23)/Fidelity (21) between the reconstructed state and that of the ideal.

We return now to the dialogue. Due to the mentioned limitations of process tomography, recent literature has risen seeking methods to quickly judge whether a quantum circuit is within tolerance

⁹ Two common ways of turning the Fidelity into a metric are the *Bures metric*, $B(\rho, \sigma) \equiv \sqrt{2 - 2\sqrt{F(\rho, \sigma)}}$ and the *angle*, $A(\rho, \sigma) \equiv \arccos(\sqrt{F(\rho, \sigma)})$, a very comprehensive discussion of these details can be found elsewhere, e.g. Ref. [34].

required for successful application, such as Bowdrey et. al. [36], and later Nielsen [32]. Of particular interest to our goal is the work by Gilchrist, Langford, and Nielsen [34]. This paper influenced our point of view by presenting a logical set of Axioms that an error measure Δ between the real process $\mathcal{F}(\psi)$ and ideal process $\mathcal{E}(\psi)$ should adhere to. They developed criteria allowing experimentalists to avoid full process tomography by applying "distance measures" between the circuit's response to a set of input states forming a complete operator basis [34], as opposed to reconstructing the operator in full process tomography. This is done by comparing the real process $\mathcal{F}(\psi)$ with the ideal process $\mathcal{E}(\psi)$ while keeping track of the worst case Trace Distance (*S-Distance*) and worst case Fidelity (*S-Fidelity*) for all considered input states. In light of a "gold standard"¹⁰ Ref. [34] stated that, "...the *S-Distance* and *S-Fidelity* are the two best error measures, and should be used as the basis for comparison of real quantum information processing experiments to the theoretical ideal."

Before proceeding to Sec. 3 for a discussion of quantum fault models, this section is concluded by mentioning that the current methods of quantum process validation (as applied to switching networks) are classically equivalent to keeping track of the largest variance from the nominal voltage response for a complete set of input states. Although this is a practical way to test small switching networks, in the future it will become intractable as it did classically, when the early days of *ad hoc* validation were aimed at exhaustively filling in the entries of a truth table.

3 Quantum Fault Models

The purpose of this section is twofold. The first is to connect the abstract concept of quantum evolution with gate level functional fault models. The second and main purpose of this section is to introduce a set of physically motivated Axioms believed to adequately capture the nature of faults inherent in quantum circuits (built with k -CN gates). Developing a test set completely satisfying these Axioms enables the elimination of many unnecessary input patterns that *a priori* appear highly plausible.

To separate the general from the particular, a focus is made on error and fault models that are independent of implementation and dependent on the quantum circuit. However, information cannot exist without a physical representation. Thus, without loss of generality we employ examples from liquid state nuclear magnetic resonance spectroscopy (NMR)¹¹ and optical quantum computation. Since the NMR implementation is currently the most successful [37] it therefore offers insight into the types of problems that may occur in a robust implementation. On the other hand, although optical networks offer a lower qubit count, most engineers are already familiar with the principles of classical optics, and the state and process tomography methods are simpler and well understood, see [28][38].

NMR exploits the ability of the spin active nuclei in molecules of a liquid sample decoupling from each other and therefore being separately addressable. When a nucleus is placed in a magnetic field the spin will be quantized and transitions between quantization levels can be induced by oscillating the field with a given resonance frequency [39]. Strong superconducting magnets are used to generate the field oscillation in the radio frequency (RF) band [39]. The most important nuclei are spin($\frac{1}{2}$) systems. Given the arbitrary assignment of $|0\rangle$ to spin up ($+z$) and $|1\rangle$ to spin down ($-z$), one may consider spin($\frac{1}{2}$) nuclei analogous to bits in a digital computer.

Each nuclear spin may thus act as a separate addressable qubit, and each molecule as a separate few-qubit quantum computer. The original interests in NMR was from chemists. They relied on the chemical shift present in the electron cloud around the nucleus (along with the J-coupling interaction between spins) as a powerful method of insight into molecular structure [39]. The first time these (or any) quantum mechanical properties were harnessed to compute information took place around August 1st in 1998 when J. A. Jones and M. Mosca implemented Deutsch's algorithm on a two qubit NMR quantum computer based on the small molecule cytosine [41]. NMR has since progressed to control on the order of ~ 7 bit coherent quantum evolution, thereby enabling many small quantum computations to be successfully realized [42].

Optical quantum computation has also recently made progress. In 2003 O'Brien et al. successfully demonstrated an all-optical quantum CN gate [43]. This gate was improved and further characterized in 2004 by both O'Brien et al. [28] and White et al. [38]. In an optical system, qubits are realized via photon polarizations. Given the arbitrary assignment of $|\leftrightarrow\rangle$ to basis $|0\rangle$ (Horizontal) and $|\updownarrow\rangle$ to basis $|1\rangle$

¹⁰ Given in Ref. [34] is the notion of a "gold standard" for quantum information processing. A "gold standard" is a single measure of distance Δ that may be used to compare and contrast a real process \mathcal{F} and an ideal process \mathcal{E} , $\Delta(\mathcal{F}, \mathcal{E})$.

¹¹ See Jones [39] for an introduction geared towards those new to NMR Quantum Computing.

(Vertical), one may consider photon polarization states as that required for qubit realization.¹² Optical networks represent physical sequences of gates. This lends well to the ideas of classical test, wherein a fault is space time invariant. Furthermore, the ideas of classical noise impacting a signal during propagation can be viewed as unwanted perturbation acting on the photons during their journey through the circuit.

Despite these rapid advancements, optical networks are currently limited to ~ 2 qubits and none of the quantum mechanical information processing systems available today are robust enough to solve problems of any interest. Quantum systems will one day become large scale. Verification techniques need to be well established to detect and diagnose improper functions. The presented fault models will allow researchers to approach the quantum test problem from testing the gate level function of all network components.

An example of a gates' structure dependent function is a *yes/no* ability to send the phase of the target backwards to the controls a tolerable percentage of the time. For example, consider the case that an otherwise functional CN gate may not adequately send phase backwards. A quantum test engineer must develop a complete test set (that is ideally minimal) to show that this fault is not present. Such a test set is complete, if it illustrates the gate's ability to send phase backwards from target to control, as previously explained in Sec. 1.2. Repeating this test set many times—as *in an ensemble*—allows one to sample over the ability of the gate to send phase backwards.

Each element in a quantum test set is an initial state and observable pair. Consider now a functional test set for the CN gate:

$$\begin{aligned} T = \{t_0, t_1, t_2, t_3, t_4, t_5\} = \\ \{ \{ |\mp\rangle \otimes |1\rangle, \hat{\mathcal{B}} \}, \{ |\pm\rangle \otimes |0\rangle, \hat{\mathcal{B}} \}, \\ \{ |-\rangle \otimes |-\rangle, \hat{X} \}, \{ |+\rangle \otimes |-\rangle, \hat{X} \}, \\ \{ |-\rangle \otimes |+\rangle, \hat{X} \}, \{ |+\rangle \otimes |+\rangle, \hat{X} \} \end{aligned} \quad (26)$$

where $\hat{\mathcal{B}}$ is a measurement in the Bell Basis [22] and $\sigma_x^{\otimes 2} = \hat{X}$. Test t_0 concurrently examines the gate's on and off action provided basis input $|1\rangle$ in addition to the controls' impact on both basis states. Test t_1 is similar to test t_0 except now the gate is toggled with the target state in basis $|0\rangle$. The gate has now acted on all (classical) basis states. Test t_2 and t_3 determine if the gate exhibits correct backwards phase traversal. Test t_4 determines if any phase crosstalk occurs such that the phase of the control impacts the phase of the target. Test t_5 determines if any relative dephasing between the target and control takes place. As an alternative to the measurement observables defined in T , each initial state may be reconstructed with state tomography and compared to the ideal via the Trace Distance and the Fidelity measures. For example t_0 and t_1 allow the calculation of what we will call the *Gate-on/off-Fidelity*, t_2 and t_3 allow calculation of the *Phase-Kickback-Fidelity*, test t_4 allows calculation of the *Phase-Crosstalk-Fidelity* and using test t_5 the *Relative-Phase-Damping* may be determined. Phase faults are better described in Sec. 3.3. We have thus completely characterized the function of the CN gate as illustrated in the truth table in Fig. 3 and can thereby infer correct function.

$ a\rangle$	$ b\rangle$	$ p\rangle$	$ q\rangle$
$ 0\rangle$	$ 0\rangle$	$ 0\rangle$	$ 0\rangle$
$ 0\rangle$	$ 1\rangle$	$ 0\rangle$	$ 1\rangle$
$ 1\rangle$	$ 0\rangle$	$ 1\rangle$	$ 1\rangle$
$ 1\rangle$	$ 1\rangle$	$ 1\rangle$	$ 0\rangle$
$ +\rangle$	$ +\rangle$	$ +\rangle$	$ +\rangle$
$ -\rangle$	$ +\rangle$	$ -\rangle$	$ +\rangle$
$ +\rangle$	$ -\rangle$	$ -\rangle$	$ -\rangle$
$ -\rangle$	$ -\rangle$	$ +\rangle$	$ -\rangle$

Fig. 3 CN Gate Truth Table for a Complete (bi-orthogonal) Functional Operator Basis. (“*The Computational*,” and “*Conjugate Basis* [30].”)

Aside from the gate level functional fault models that will be introduced, we consider the case of random and systematic errors as they appear in the current literature.¹³ Since quantum noise is randomly

¹² All possible pure polarization states may be constructed from coherent superpositions of these two states: For example, diagonal, anti-diagonal, right-circular and left-circular polarized light are respectively represented by, $|D\rangle = |\nearrow\rangle = (|\leftrightarrow\rangle + |\updownarrow\rangle)$, $|A\rangle = |\swarrow\rangle = (|\leftrightarrow\rangle - |\updownarrow\rangle)$, $|R\rangle = (|\leftrightarrow\rangle + i|\updownarrow\rangle)$ and $|L\rangle = (|\leftrightarrow\rangle - i|\updownarrow\rangle)$.

¹³ Without loss of generality local Markovian noise models are considered.

distributed, a complete test set must adequately sample its uniform impact. Circuit locations impacted by random and systematic errors must now be defined.

In quantum error correcting codes, fault locations are between circuit stages,¹⁴ and have quantifiable error probabilities or strengths of occurrence [45]. For example, consider the five stage circuit shown in Fig. 4. The numbered locations of possible gate external faults are illustrated by placing an "x" on the line representing a qubits time traversal and here, the five gates, initial states ($|i_0\rangle, |i_1\rangle, |i_2\rangle$) and measurements (m_0, m_1, m_2) may also contain errors. Next definitions of some terms used throughout this section are given:

Definition 5 *Error Location:* The wire locations between stages as well as any node or gate in a given network (see Fig. 4).

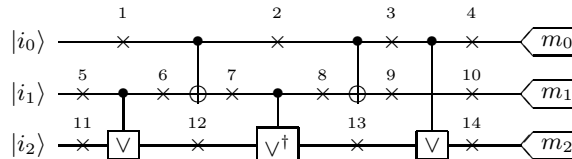


Fig. 4 2–CN (2–CN) gate with 14 gate external error locations numbered above an "x" and five possibly erroneous gates. (The construction of the gates used in this circuit are outlined in Sec. 3.4.)

Definition 6 *Gold Circuit:* A quantum circuit denoted GC defining a standard by operating in the ideal. Typically a non-ideal quantum circuit is denoted QC .

It is the goal of this paper to develop fault models that sample failure rates. We therefore consider a set of error models adequately capturing the nature of fault types occurring in a given circuit, together with their locations.

Definition 7 *Fault Set:* Denote by F_q a set containing all considered faults assumed to impact QC .

We introduce the concept of what will be called the *quantum single fault model*. This allows researchers using the defined fault models to consider separately all errors at each location for a given quantum circuit. We present first Def. 8 and next Conjecture 1, both related to this idea.

Definition 8 *Quantum Single Fault Model:* For simplification the "quantum single fault model" is introduced in this work. Consider the fault set F_q . In the single fault model, test plans are optimized for all $f \in F_q$ assuming that only a single f perturbs QC exclusively. Multiple faults perturbing QC will accumulate and be detected, but the single fault model makes it much easier to develop test plans.

Conjecture 1 A test set designed to detect all considered single errors will detect and sample the accumulated impact of multiple errors at multiple locations.

A quantum test set is a set of initial state and measurement pairs designed to drive a network to threshold limits. For example, one may develop a test set that first turns as many gates on as possible, next turns the highest possible number of gates off and then sends phase through as many gates during one test as the structure of the network would allow.

Definition 9 *Quantum Test Set:* A sequence of initial states $|\psi_i\rangle$ and measurements M_m denoted as $T_i = \{|\psi_i\rangle, M_m\}$ used to distinguish QC possibly perturbed by any $f \in F_q$ from a gold circuit GC .

Complete fault coverage occurs after a test set has determined that the considered fault(s) are not physically present in a given circuit.

Definition 10 *Fault Coverage:* Denote by QC a quantum circuit possibly perturbed by any element of a set of faults $f \in F_q$ and a test set T_i complete for all $f \in F_i$. Fault Coverage occurs for fault $f \in F_q$ by experimentally running $t \in T_i$ that samples f . A quantum test pattern that detects (covers) all $f \in F_q$ is called a complete test set. A complete test set with the fewest test vectors is called minimal.

With the basic definitions behind us, the coming subsections discuss gate level errors and introduce several Axioms. These Axioms act as functional, gate level fault models. Each Axiom must be satisfied by some element(s) of a test set in order to cover all considered faults.

¹⁴ In particular see [45] where, in that early work, Knill, Laflamme, and Zurek justified the idea of an error location for the purpose of quantum error correction.

3.1 Pauli Faults

Quantum computation involves manipulating coherent superpositions [44]. These superpositions are described as fragile by several authors including Shor [44], Amin et. al. [9], Knill, Laflamme and Zurek [45], and are naturally prone to several types of failures. Decoherence destroys the information contained in the superposition possible among qubits [44][46]. Its typical form in NMR is known as *spin-spin* and *spin-lattice* relaxation [47]. Decoherence is typically thought of as the environment constantly measuring a quantum system though interacting with it [48]. To model this impact, one may adopt what is known as the partial trace.

For example, consider ρ_e from Eqn. 6. Now assume our quantum computer was only a single bit device that became entangled somehow with an environment represented by the second qubit. Unbeknownst to us, the second qubit is implicitly measured at a later time, altering the state of the first. To model this impact, one will trace over the second qubit,¹⁵ leaving the first qubit in a mixed state. To do this, define first a basis to perform the trace with respect to:

$$|e_i\rangle \implies \begin{cases} |e_0\rangle = |0\rangle, & i = 0 \\ |e_1\rangle = |1\rangle, & i = 1 \end{cases} \quad (27a)$$

$$(27b)$$

Now sum over the inner products of the quantum state and the basis formed by $|e_i\rangle$, like this:

$$\text{tr}_2(\rho_e) = \sum_i \langle e_i | \rho_e | e_i \rangle = (\sigma_i \otimes \langle 0 |) \cdot \rho_e \cdot (\sigma_i \otimes |0\rangle) + (\sigma_i \otimes \langle 1 |) \cdot \rho_e \cdot (\sigma_i \otimes |1\rangle) = \frac{1}{2} (|0\rangle \langle 0| + |1\rangle \langle 1|). \quad (28)$$

The state of the first qubit is now assumed randomized as shown in Eqn. 28.

This entanglement of a quantum processor with the outside world [45] is described by many authors including [49] as, "*coupling to an initially independent environment.*" A large amount of research has been devoted to impeding decoherence by means of quantum error correcting codes. Consequently, common fault models are found in the quantum error correcting code literature [44][50][51][52][53]. The most investigated error model is known as an "*independent depolarizing error* [45]." This model has the effect of completely randomizing a given qubit with some probability p [22]. "*Error models designed to control depolarizing errors apply to all independent error models* [49]." These codes are designed to correct unwanted occurrences of the Pauli Spin Matrices. The following is a list of the wide range of errors modeled assuming Pauli Faults, with some supporting references:

1. Depolarizing Channels [22][49]
2. Amplitude Dampening [22][45]
3. Phase Damping [22][54]
4. Phase-Flips [22][45][54]
5. Bit-Flips [22][45]
6. Initialization Inaccuracies [54][55]
7. Measurement Inaccuracies [31][56][57]

Definition 11 *Pauli Fault Model: The addition of an unwanted Pauli matrix f in quantum network QC, at error location l and with placement probability p . The Pauli matrices are given in Eqn. 16, 17 and 18.*

A large variety of potential error sources must be circumvented in any physical implementation. For example, in NMR pulses must be 'shaped' or tailored to physical parameters of the individual molecules in the sample. Proper RF coil homogeneity is crucial in avoiding excessive signal attenuation [47] and in quantum optical circuits, "*...the imperfect mode matching of the interferometers...* [28]" lead to reproducible errors. The types of errors associated with physical construction lead to another class of faults addressed in the literature, known as *systematic errors*. Systematic errors are closer to the types of errors that classical test engineers refer to as faults.¹⁶ An introduction to some of the most common systematic errors will be given in the next three paragraphs. These errors are described by Cummins and Jones as, "*arising from the reproducible imperfections in the apparatus used to implement quantum computations* [58]." These types of errors are very generally modeled by inserting Eqns. 29, 30 and 31 into error locations as done with Pauli Faults. The difference is that instead of a Pauli Fault occurring with a given probability, these inaccuracies occur with a gaussian distribution of angle θ and accumulate throughout the computation [44]. (These will be referred to as Rotational Faults and modeled using Eqns. 29, 30 and

¹⁵ The partial trace is further discussed in Appendix A.

¹⁶ *Interesting Fact:* In NMR quantum computing [62] it is well known that both the air conditioner in the room, and the quantum computer's power supply have periodic impact on a circuit's function. The time between cycles is around 20 minutes as opposed to the very short time allowed for current quantum circuits to be run.

31. However, Theorem 1 relates the Rotational and Pauli Fault models.) The most advanced research regarding these failures is found in NMR literature [35][47][58], however similar forms of these error types are found in all quantum circuit realization technologies.

$$R_x(\theta) = \begin{pmatrix} \cos(\theta/2) & -i \cdot \sin(\theta/2) \\ -i \cdot \sin(\theta/2) & \cos(\theta/2) \end{pmatrix} \quad (29)$$

$$R_y(\theta) = \begin{pmatrix} \cos(\theta/2) & -\sin(\theta/2) \\ \sin(\theta/2) & \cos(\theta/2) \end{pmatrix} \quad (30)$$

$$R_z(\phi) = e^{-i\phi/2} |0\rangle\langle 0| + e^{i\phi/2} |1\rangle\langle 1| \quad (31)$$

Systematic Pulse Length Errors In NMR gates are created by making adjustments to a Hamiltonian similar to Eqn. 32 thereby addressing the nuclear spins of the sample by time dependent RF pulses. These adjustments allow for the controlled change of the state of qubits.¹⁷

$$\hat{H} = \sum_{i,\alpha} \alpha_{i\alpha} \sigma_{i\alpha} + \sum_{i,j} J_{ij} \sigma_{i\alpha} \sigma_{j\alpha} \quad (32)$$

Eqn. 32 contains a term for individual bitwise operations, $R_{i,\alpha}(\theta) = e^{-i\frac{\theta}{2}\sigma_{i\alpha}}$ and an interaction (*Ising*) term $J_{ij}(\phi) = e^{-i\frac{\phi}{2}\sigma_{i\alpha}\sigma_{j\alpha}}$ to allow entanglement between qubits and is thus general [59]. Controlling the Hamiltonian in Eqn. 32 results in pulse length errors since a machine is never able to supply infinite precision regarding continuous parameters [35]. A goal of developing test plans is to show experimentally that these inaccuracies are small enough to be tolerated. The accuracy of a machine's ability to translate one state to another depends on the NMR Rotor Fidelity.¹⁸ Bowdrey and Jones [35] have given a simple measure of NMR Rotor Fidelity. (Trapped Ion quantum computers also suffer from a similar error in the inaccuracies of the applied laser [63]). In NMR literature, pulse length errors are described as, "the machine not being set correctly [58]," or when the applied RF field deviates from its nominal value, known as, "spatial inhomogeneity [58]." Even if the implementation does not rely on a time controlled Hamiltonian [59], one may still consider something very similar to pulse length errors as: "...imprecise unitary operations acting on the system and accumulating over the computation [45][44]."

Systematic Off-Resonance Effects Each spin nuclei in an NMR sample may be addressed via an individual resonant frequency in terms of an electromagnetic pulse. Simultaneous (as opposed to consecutive) pulses at two or more nearby frequencies are desirable to shorten sequences, yet transient phase shifts (\sim tens of degrees) greatly deteriorate such simultaneous rotations [58][35][47].¹⁹ Cummins and Jones formally describe this as, "...off resonance effects [in NMR quantum computation] arise from the use of a single RF source to excite transitions in two or more spins which have different resonance frequencies... [58]." Independent of any particular implementation, these errors are modeled by considering all unwanted rotations given in Eqns. 29, 30 and 31.

Systematic Refocusing Errors Quantum operations designed to impact a component subset of qubits in a quantum register inadvertently impact composite qubits. Refocusing [64] is a procedure that allows correction for this unwanted impact. In terms of NMR, "the unselected spins must not be affected by the RF irradiation [47]." This can result in substantial (\sim tens of degrees) phase shifts of neighboring unaddressed spins [47]. Very generally, these errors are modeled by considering all of the unwanted rotations given in Eqns. 29, 30 and 31.

This concludes our introduction to the wide range of errors modeled with Pauli Faults. Before proceeding to Sec. 3.2 two Axioms that quantum test sets must satisfy are given. Axioms 1 and 2 provide necessary and sufficient conditions for a test set T_i to be complete for the Pauli Fault Model.

Quantum Test Axiom 1 *A bit flip (σ_x or σ_y) at any error location must be detectable. ■*

Quantum Test Axiom 2 *A phase flip (σ_z or σ_y) at any error location must be detectable. ■*

¹⁷ The timed "evolution" of a quantum system is governed by the Schrödinger equation [60], and controlled by the Hamiltonian represented as \hat{H} .

¹⁸ A general or universal NMR rotor translates any state independent of the initial spin [58] using what are known as composite pulses [61].

¹⁹ Called "Bloch-Siegert effects" or "transient Bloch-Siegert effects" in NMR, see [47].

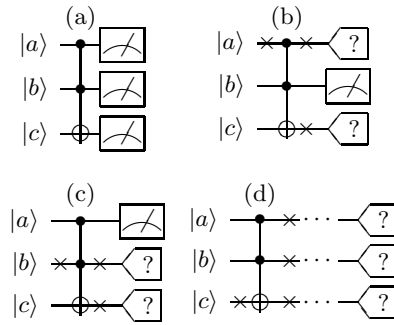

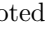
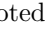


Fig. 5 Initialization Errors Impacting a 2–CN Gate: (a) correct circuit, (b)-(d) various initialization errors.

3.2 Initialization Errors

Initialization faults were discussed in detail by Kak [54], and addressed experimentally in [55].²⁰ Of particular support to our idea of quantum test set generation is Kak’s claim that certain initialization errors are very difficult to circumvent via error correcting codes. Because initialization accuracies relate to a machine’s ability to perform a task (such as not permuting the initial state population in NMR [47]), this supports well the idea of using a test set to determine if the machine is functional before we rely on the quantum computer to solve a problem of interest. These faults are modeled next in Def. 12, by assuming that they are independent and uncorrelated.

Definition 12 *Initialization Error: A qubit with an initial state differing from the ideal due to the addition of a rotation $R_n(\theta)$ where $n \in \{x, y, z\}$, around one axis of the Bloch Sphere, or a qubit that statistically favors correct preparation in one basis state over the other.*

Considering Def. 12, contrived examples of how initialization faults spread are shown in Fig. 5. Correct measurements are illustrated by drawing a  to the right of the circuit. In Fig. 5 (a) three functional measurement gates are shown and one finds the first example of a fault in Fig. 5 (b). This could occur when the desired initial state is $|01c\rangle$ and the top qubit is rotated around the x axis (inverting $|c\rangle \rightarrow |\bar{c}\rangle$) and resulting in state $\cos\theta|01c\rangle - i\sin\theta|11\bar{c}\rangle$. After passing through the 2–CN gate, the state of the system becomes $\cos\theta|01c\rangle - i\sin\theta|11c\rangle$. There is now a probability of $(\sin\theta)^2$ that an incorrect value will be measured.²¹ This uncertainty is denoted by replacing  symbols with .

A similar scenario holds for Fig. 5 (c), the difference is that the center qubit is impacted by an initialization fault as opposed to the top qubit in Fig. 5 (b). In Fig. 5 (d), suppose that the desired initial state of the register is $|--+\rangle$, however an error impacts the bottom qubit such that its phase is flipped. This results in the incorrect initial state of $|---\rangle$. Now the 2–CN gate will entangle the state of the system incorrectly, resulting in state $(|00\rangle - |01\rangle - |10\rangle - |11\rangle)|-\rangle$. This fault can be detected with a test set detecting unwanted instances of the Pauli Faults at the start of the circuit—sufficiently addressed in Axioms 1 and 2. A second type of initialization error will now be discussed.

Generally, there exists a certain set of states left invariant under a quantum operation [22]. For example, qubit preparation may be permuted with a form of amplitude dampening. Thus, a qubit may have favored preparation in one state over the other. A qubit that favors preparation in state $|0\rangle\langle 0|$ is modeled with the following operation elements:

$$E_0 = |0\rangle\langle 0| + \left(\sqrt{1-\gamma}\right) |1\rangle\langle 1| \quad (33)$$

$$E_1 = |0\rangle\langle 0| + (\sqrt{\gamma}) |1\rangle\langle 1| \quad (34)$$

Consider a register prepared in density state matrix $\rho = \rho_0 \otimes \dots \otimes \rho_k \otimes \dots \otimes \rho_n$. The k^{th} qubit is desired to start the computation in an arbitrary state, expressed as:

$$\rho = \rho_0 \otimes \dots \otimes \begin{pmatrix} \alpha^2 & \alpha\beta^* \\ \beta\alpha^* & \beta^2 \end{pmatrix} \otimes \dots \otimes \rho_n \quad (35)$$

²⁰ In NMR, temporal and spatial averaging have been the most popular choices for preparing effective pure states [47].

²¹ This example illustrates the fact that an initialization error will not grow in an otherwise ideal quantum mechanical computation as noted by Zurek [65] in 1984.

The unwanted impact of initial state dampening is expressed as: $\mathcal{E}(\rho) = \sum_k I \otimes \dots \otimes E_k \otimes \dots \otimes I \cdot \rho \cdot I \otimes \dots \otimes E_k^\dagger \otimes \dots \otimes I$. This results in the state:

$$\rho' = \rho_0 \otimes \dots \otimes \begin{pmatrix} \alpha^2 + \gamma\beta^2 & \alpha\beta^*\sqrt{1-\gamma} \\ \beta\alpha^2\sqrt{1-\gamma} & \beta^2(1-\gamma) \end{pmatrix} \otimes \dots \otimes \rho_n \quad (36)$$

The portion of the k^{th} qubit's superposition in basis state $|1\rangle \langle 1|$ is forced into basis state $|0\rangle \langle 0|$ and the interfering terms are suppressed (both based on some parameter γ). Similarly, a qubit may also favor preparation into state $|1\rangle \langle 1|$. Axiom 3 is logically justified by considering the case that a qubit favors correct preparation in basis states $|0\rangle$ or $|1\rangle$.

Quantum Test Axiom 3 *Each qubit must be initialized in both basis states $|0\rangle$ and $|1\rangle$.* ■

3.3 Lost Phase Faults

Shenvi, Brown and Whaley [53] studied Grover's search algorithm [22] impacted by a random phase error in the oracle.²² Their work addressed the complexity of finding a solution to the search problem impacted by quantum noise. They model these errors by applying a certain unwanted phase $\pm\epsilon$ to the state of a quantum register marked by an oracle:

$$\mathcal{O} : |k\rangle \longrightarrow (-1)^{f(k\pm\epsilon)} |k\rangle, \quad (37)$$

this is referred to classically, as "fault-simulation." Several references including [53] call this a "phase-kick-error." In this work we present Fig. 6 (b), (c) and (d) to illustrate the idea that one of the controls in a given gate is not functioning and therefore will not exhibit correct phase kick-back behavior. There are two related Axioms introduced in this section. The first of which is intended to test phase kickback, while the second is intended to account for unwanted phase swap and relative phase damping.

Quantum Test Axiom 4 *Provided the state of the target is $|-\rangle$: Each gate must be shown to attach a relative phase to an arbitrary activating state $|a\rangle$ with both positive and negative eigenvalues. Furthermore, each gate must be shown not to attach a relative phase to arbitrary non-activating state $|n\rangle$ with both positive and negative eigenvalues. The target state must remain globally invariant under both $|a\rangle$ and $|n\rangle$.* ■

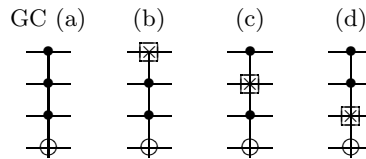


Fig. 6 3–CN Gate and Phase Faults: (a) Gold Circuit (GC), (b) Weak top control, (c) Weak second control, (d) Weak bottom control.

Phase damping is a noise process altering relative phases between states [22]. The next Axiom is designed to determine if any gates in the network apply unwanted relative phase shifts or unwanted phase swaps between target and control.

Quantum Test Axiom 5 *Provided the state of the target is $|+\rangle$: relative phase must be shown not to change under arbitrary activating state $|a\rangle$ with both positive and negative eigenvalues. Furthermore, relative phase must not change under arbitrary non-activating state $|n\rangle$ with both positive and negative eigenvalues.* ■

²² Grover's original algorithm under the impact of noise addressed in [53] has recently been updated by L. Grover [66]. Although this new "Fixed Point Algorithm" is more robust, it of course is still subject to phase errors (no modification of the oracle took place). The algorithm has been experimentally verified in the recent preprint by Li Xiao and J. A. Jones [67], systematic errors in the physical implementation were briefly explored. B. Reichardt and L. Grover have also recently developed methods of systematic error correction for this new algorithm [68].

A functional 3–CN gate will map an input state $|++\rangle|-\rangle$ into the output state $(|000\rangle + |001\rangle + |010\rangle + |011\rangle + |100\rangle + |101\rangle + |110\rangle - |111\rangle)|-\rangle$. Here, it must be pointed out that each true minterm in the superposition that activates the control gate will undergo a phase shift of $|n\rangle \rightarrow e^{i\pi}|n\rangle$, as shown by the $-|111\rangle$ term above. Similar ideas will be used to detect faults. For example, if the fault in Fig. 6 (b) is present, the circuit’s response may be $(|000\rangle + |001\rangle + |010\rangle - |011\rangle + |100\rangle + |101\rangle + |110\rangle - |111\rangle)|-\rangle$. If such is the case, negative phase is assigned to both $|011\rangle$ and $|111\rangle$ since those both activate the gate (now that the top control is broken).

This section is concluded by mentioning that, under the influence of the considered faults, information will be encoded in the phase of the superposition output state that represents the function of the circuit. Phase is negated for every superposition state that represents a minterm of the function. The Phase of states that do not represent true minterms is left invariant. The goal of the quantum test engineer is to develop a complete and minimal test set to extract this functional information.

3.4 Faded Control Faults

Aside from the phase properties discussed prior to this section (3.3), suitable Hamiltonians must be sequenced to correctly create control gates which act properly (non-inclusively of course) on classical n –dimensional basis input state vectors:

$$|\psi_b\rangle = \{|0\rangle, |1\rangle\}^{\otimes n}. \quad (38)$$

The building blocks needed to implement any quantum algorithm with NMR can be based on single spin rotations and CN gates [47]. CN gates are realized using a scheme similar to that given in Fig. 7, where the center gate is called a CZ gate (built using a ϕ gate with angle π , see [69], § 3.1 Eqn. 34), taking an ideal form:

$$CZ_i = |00\rangle\langle 00| + |01\rangle\langle 01| + |10\rangle\langle 10| + e^{i\pi}|11\rangle\langle 11|. \quad (39)$$

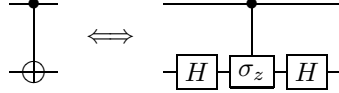


Fig. 7 CN gate constructed with elementary building blocks [69]. The H gate ($H = iR_y(\pi/2)R_z(\pi)$) is given as $H = \frac{1}{\sqrt{2}}(|0\rangle + |1\rangle)\langle 0| + \frac{1}{\sqrt{2}}(|0\rangle - |1\rangle)\langle 1|$ and the center controlled phase shift gate (CZ_i) is given in Eqn. 39.

Of course, in any physical implementation, quantum logic gates are never nominal. The CZ_i gate deviates according to our ability to apply phase $e^{i\phi}$ correctly to term $|11\rangle\langle 11|$. This can be represented as:

$$CZ_r = |00\rangle\langle 00| + |01\rangle\langle 01| + |10\rangle\langle 10| + e^{i\phi}|11\rangle\langle 11|. \quad (40)$$

Assuming no other gate is dysfunctional, return to Fig. 7 observing that an ideal CN gate creates the following mapping: $CN_i : |10\rangle \rightarrow |11\rangle$. In the presence of the network’s inability to supply phase at a correct angle ϕ , the mapping becomes: $CN_r : |10\rangle \rightarrow (1 + e^{i\phi})|10\rangle + (1 - e^{i\phi})|11\rangle$. The fidelity between the real and ideal CN gate is easily calculated to be:

$$F(CN_i |10\rangle, CN_r |10\rangle) = \frac{1}{2}(1 - \cos\phi). \quad (41)$$

A second common operation constructed similarly to a CN gate (using a ϕ gate with angle $\pi/2$ [69]) is known as the CV gate. The V gate (known as the square root of NOT, often denoted \sqrt{NOT}) is given as:

$$V = |V_0\rangle\langle 0| + |V_1\rangle\langle 1|, \quad (42)$$

where $|V_0\rangle = (1 + i)|0\rangle + (1 - i)|1\rangle$ and $|V_1\rangle = (1 - i)|0\rangle + (1 + i)|1\rangle$. The CN and CV gates may be combined to create 2–CN gates as shown in Fig. 8. It turns out that by adjusting ϕ , n^{th} root of NOT gates can be constructed [27]. These can be used to build any k –CN gate (by setting $\phi = \pm\pi/4$ the 4th root of NOT gates can be created and used to build the 3–CN gates in this paper).

Test sets complete for the faded control fault model concurrently activate all controls.²³ These test sets also address each control with a non-activating state, as can be seen in Fig. 9. This allows one to

²³ In classical logic a similar fault model could arise when an AND gate is dysfunctional [21].

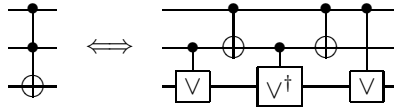


Fig. 8 2-CN (2-CN) gate constructed with elementary building blocks.

determine the controls’ correct function with the target in a basis state. It also tests the controls’ impact on both activating and non-activating states. This subsection concludes by presenting Axiom 6. Sec. 3.5 continues the gate level fault discussion.

Quantum Test Axiom 6 *For the target acting separately on basis state $|0\rangle$ and $|1\rangle$: All controls must be activated concurrently. Furthermore, each control must be addressed with a non-activating state. ■*

input	GC(a)	b	c	d	input	GC(a)	b	c	d
$ 0\rangle$	0	0	0	0	$ 8\rangle$	8	8	8	8
$ 1\rangle$	1	1	1	1	$ 9\rangle$	9	9	9	9
$ 2\rangle$	2	2	2	2	$ 10\rangle$	10	10	10	10
$ 3\rangle$	3	3	3	11	$ 11\rangle$	11	11	11	3
$ 4\rangle$	4	4	4	4	$ 12\rangle$	12	12	12	12
$ 5\rangle$	5	5	13	5	$ 13\rangle$	13	13	5	13
$ 6\rangle$	6	14	6	6	$ 14\rangle$	14	6	14	14
$ 7\rangle$	15	15	15	15	$ 15\rangle$	7	7	7	7

Fig. 9 Truth Table containing decimal entries for the 3-CN Gate Impacted by Missing Control Faults. The column denoted 'input' shows the input combinations possible on the amplitude plane where GC denotes the correct response. Columns denoted 'b' to 'd' illustrate the circuit’s response given the presence of faults from Fig. 6 (b) through (d).

3.5 Forced Gate Faults

In the most general case, quantum circuits are *wired* together using direct field interactions and *gates* are built by applying a force. Any quantum algorithm may be depicted as a sequence of unitary transformations represented as rotations in a Hilbert space. In NMR, "...examples of unitary transformations are evolution during RF pulses and free evolution under the system Hamiltonian... [47]." In practice, "non-qubit degrees of freedom are possible [70]" and experimentally quantum gates perform a process which approximates the desired unitary operation, that adds decoherence [22]. (In NMR, "...relaxation processes give rise to non-unitary transformations [47]...") A complete test set for the fault model presented in Fig. 10 forces each gate in a binary quantum network to act on both basis input states $|0\rangle$ and $|1\rangle$. This can be seen further by examining the Truth Table in Fig. 11. The Forced Gate Fault model is given in Fig. 10.

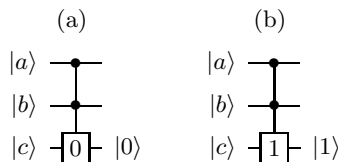


Fig. 10 Forced gate Faults: (a) A 2-CN gate that favors correctly acting on a $|1\rangle$ by changing the state to $|0\rangle$, (b) A 2-CN gate that favors acting on a $|0\rangle$ by changing the state to $|1\rangle$. (Both of these show the state response assuming only binary inputs.)

A brief (and simple) mathematical explanation of how one would model non-unitary computations is given next: If a quantum computer is wanted to perform computations in Hilbert space $\mathcal{A} \in \mathcal{H}$ of dimension w , yet the system is housed in Hilbert space $\mathcal{B} \in \mathcal{H}$ with dimension l , a non-ideal composite computational space $\mathcal{A} \otimes \mathcal{B}$ will result with dimension w product l . Of course, \mathcal{B} does not form a space for any meaningful computations, however, \mathcal{B} is controllable to the point that any initial state $|e_i\rangle \in \mathcal{B}$ is pure.

<i>input</i>	GC	a	b
000⟩	000	000	000
001⟩	001	001	001
010⟩	010	010	010
011⟩	011	011	011
100⟩	100	100	100
101⟩	101	101	101
110⟩	111	110	111
111⟩	110	110	111

Fig. 11 The Truth Table for 2–CN Gate and the impact of Forced Gate Faults: The column denoted 'input' shows the respective input combinations possible on the amplitude plane. Columns denoted 'a' and 'b' show the circuit's response given the presence of faults from Fig. 10 (a) and (b).

<i>input</i>	a	b
000⟩	0	0
001⟩	0	0
010⟩	0	0
011⟩	0	0
100⟩	0	0
101⟩	0	0
110⟩	1	0
111⟩	0	1


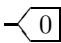
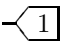
Fig. 12 Fault Table for 2–CN Gate perturbed by the Forced Gate Faults given in Fig. 10. Each binary entry in the fault table corresponds to a single test (row) and a single fault (column). Tests are labeled |000⟩ to |111⟩ and faults are labeled 'a' and 'b', as shown in Fig. 10 (a) and (b). A '1' in the table corresponds to a given test (row) detecting a given fault (column).

In order to construct an operator $U_a = \sum_i |a_i\rangle \langle a'_i|$ designed to act on space \mathcal{A} alone, one inadvertently interacts with system \mathcal{B} . The desired operator U_a becomes $U_{ab} = U_a \otimes U_b = \sum_i |a_i\rangle \langle a'_i| \otimes \sum_i |b_i\rangle \langle b'_i|$, this results in U_{ab} taking the form $\sum_i |a_i\rangle |b_i\rangle \langle a'_i| \langle b'_i|$. If one wishes to find the impact U_{ab} has on the component system of interest (any $|a\rangle \in \mathcal{A}$) a trace over the impact of system \mathcal{B} must be made. This leads to $\langle e_w | U_{ab} | e_l \rangle = \sum \langle e_w | |a_i\rangle |b_i\rangle \langle a'_i| \langle b'_i| | e_l \rangle = \sum_i |a_i\rangle \langle e_w | |b_i\rangle \langle a'_i| \langle b'_i| | e_l \rangle = \sum_i \langle e_w | |b_i\rangle \langle b'_i| | e_l \rangle |a_i\rangle \langle a'_i|$. It is now clear that U_a in general is not a unitary operator.

An example of a non-unitary operation is a gate that when activated applies an "amplitude dampening process [22]" to the target bit (a type of relaxation process [47]). Axiom 7 forces the gate to act on both a |0⟩ and a |1⟩ to uniquely show that a forced gate fault is not present. This type of fault model is called a functional fault model in classical test, as it probes the logical function of the circuit.

Quantum Test Axiom 7 *Each target must separately act on basis state inputs |0⟩ and |1⟩.* ■

3.6 Measurement Faults

Measurement faults result from a "limitation in the sensitivity of a measurement apparatus [56]." Here a faulty measurement instrument is modeled as a probe that couples to a qubit and statistically favors returning a certain value. In Fig. 13 the single measurement fault model is illustrated by placing a faulty measurement gate at the output of the circuit. Faulty measurement probes that statistically favor returning *logic-zero* are illustrated by replacing  symbols with . Similarly, probes that always return *logic-one* are illustrated with 's. The truth table derived from Fig. 13 is shown in Fig. 14.

The corresponding fault table is given in Fig. 15.

Measurement faults may also be modeled by placing unwanted Pauli Faults at the end of a circuit just before the correct measurement. For example, consider the photon polarization realization of a qubit. To project and measure the state of a photon one places a slit²⁴ in front of a photo detector. Polarization states inline with the slit will be allowed to reach the photo detector. The angle of the slit may be set as needed and this is subject to an error [31], described in [31] as, "...an uncertainty in the settings of the angles of the slit [wave-plates] used to make tomographic projection states." These faults were adequately

²⁴ A detailed discussion of errors in Photon measurement is in Ref. [31].

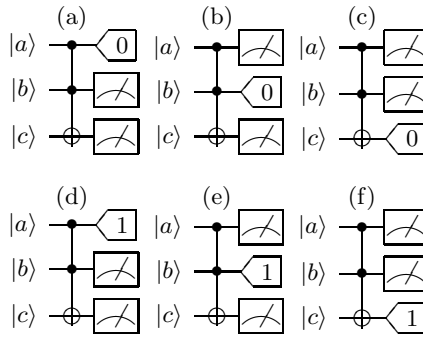


Fig. 13 Measurement Errors: Figs (a), (b) and (c) illustrate measurement faults that statistically favor *logic-zero*. Figs (d), (e) and (f) contain measurement faults statistically favoring *logic-one*.

<i>input</i>	GC	a	b	c	d	e	f
000⟩	000	000	000	000	100	010	001
001⟩	001	001	001	000	101	011	001
010⟩	010	010	000	010	110	010	011
011⟩	011	011	001	010	111	011	011
100⟩	100	000	100	100	100	110	101
101⟩	101	001	101	100	101	111	101
110⟩	111	010	100	110	110	110	111
111⟩	110	011	101	110	111	111	111

Fig. 14 Truth Table for 2–CN Gate Impacted by Measurement Faults. The column denoted 'input' shows the input combinations possible on the amplitude plane. Columns denoted 'a' through 'f' show the circuit's response given the presence of faults from Fig. 13 (a) through (f).

<i>input</i>	a	b	c	d	e	f
000⟩	0	0	0	1	1	1
001⟩	0	0	1	1	1	0
010⟩	0	1	0	1	0	1
011⟩	0	1	1	1	0	0
100⟩	1	0	0	0	1	1
101⟩	1	0	1	0	1	0
110⟩	1	1	0	0	0	1
111⟩	1	1	1	0	0	0

Fig. 15 Fault Table for 2–CN Gate Derived From Fig. 13. Each binary entry in the fault table corresponds to a single test (row) and a single fault (column). Tests are labelled |000⟩ to |111⟩ and faults are labelled 'a' through 'f'. A value of '1' in the table corresponds to a given test (row) detecting (covering) a given fault (column).

addressed in Axioms 1 and 2; the only addition that must be made models statistical inconsistency. Test sets in accordance with Axiom 8 detect the statistical faults defined in Def. 13.

Definition 13 *Measurement Fault Model:* A single functional measurement gate is replaced with a faulty measurement gate that statistically favors returning logic-zero or a logic-one.

Quantum Test Axiom 8 *Each qubit must be measured in both logic-zero and logic-one states.* ■

All the Axioms that a test set must satisfy have been introduced. This work considers the Initialization Errors (Axiom 3, Sec. 3.2) and the measurement faults (Axiom 8) discussed in this section to be largely part of the quantum computers' classical functionality. The gate level quantum faults considered were the Lost Phase Faults (Axioms 4 and 5, Sec. 3.3), Faded Control Faults (Axiom 6, Sec. 3.4), and Forced Gate Faults (Axiom 7, Sec. 3.5). In Sec. 4 conclusions will be drawn based on Axioms 1 & 2 related to the occurrence of Pauli faults.

4 Conclusions Drawn From The Pauli Fault Model

With a basic introduction to the wide range of errors addressed with the Pauli Fault Model in place, a few important properties will be discussed starting with fault domination [71]. Classically, f_2 dominates fault f_1 when the set of tests covering f_1 is included in the set of tests covering fault f_2 . Fault f_1 is therefore no longer considered. It turns out that fault domination plays an important role in quantum test engineering as well.

Input Test	σ_{x1}	σ_{y1}	σ_{z1}	σ_{x4}	σ_{y4}	σ_{z4}	σ_{x5}	σ_{y5}	σ_{z5}	σ_{x10}	σ_{y10}	σ_{z10}	σ_{x11}	σ_{y11}	σ_{z11}	σ_{x14}	σ_{y14}	σ_{z14}
{ 000⟩, Z}	p	p	0	p	p	0	p	p	0	p	p	0	p	p	0	p	p	0
{ 001⟩, Z}	p	p	0	p	p	0	p	p	0	p	p	0	p	p	0	p	p	0
{ 010⟩, Z}	p	p	0	p	p	0	p	p	0	p	p	0	p	p	0	p	p	0
{ 011⟩, Z}	p	p	0	p	p	0	p	p	0	p	p	0	p	p	0	p	p	0
{ 100⟩, Z}	p	p	0	p	p	0	p	p	0	p	p	0	p	p	0	p	p	0
{ 101⟩, Z}	p	p	0	p	p	0	p	p	0	p	p	0	p	p	0	p	p	0
{ 110⟩, Z}	p	p	0	p	p	0	p	p	0	p	p	0	p	p	0	p	p	0
{ 111⟩, Z}	p	p	0	p	p	0	p	p	0	p	p	0	p	p	0	p	p	0
{ +++⟩, X}	0	p	p	0	p	p	0	p	p	0	p	p	0	p	p	0	p	p
{ ++-⟩, X}	0	0	0	0	0	0	0	0	0	0	0	0	p	p	0	p	p	
{ +-+⟩, X}	0	p	p	0	p	p	0	p	p	0	p	p	0	p	p	0	p	p
{ +--⟩, X}	0	0	0	0	0	0	0	0	0	0	0	0	p	p	0	p	p	
{ -++⟩, X}	0	p	p	0	p	p	0	p	p	0	p	p	0	p	p	0	p	p
{ -+-⟩, X}	0	0	0	0	0	0	0	0	0	0	0	0	p	p	0	p	p	
{ --+⟩, X}	0	p	p	0	p	p	0	p	p	0	p	p	0	p	p	0	p	p
{ ---⟩, X}	0	0	0	0	0	0	0	0	0	0	0	0	p	p	0	p	p	

Fig. 16 2–CN Gate Fault Table: Generated by placing Eqns. 16 , 17 and 18 at the error locations {1,4,5,10,11,14} shown in Fig. 4 with placement probability p . Table entries correspond to the probability of observing a fault in a corresponding column under that row’s input test vector and corresponding observable, where $\sigma_z^{\otimes 3} = \hat{Z}$ and $\sigma_x^{\otimes 3} = \hat{X}$. (Preparation of superposition states and using \hat{X} observables can be done with only basis inputs and \hat{Z} observables. This is done by putting Hadamard gates on both sides of the circuit and preparing all basis inputs, each with a corresponding computational basis measurement)

In classical test there is an approach known as *constructing a fault table* used to better understand test set properties and reduce test sets. A fault table is constructed by comparing a nominal response to a circuit perturbed by each considered fault for each error location and under all input vectors. One may adapt this method to quantum test, but the table entries will typically contain probabilities [6]. Observe now the quantum fault table in Fig. 16. Each row corresponds to an initial state and observable pair (Def. 9). Each column is denoted as $\sigma_{i \times}$, where subscript i refers to a corresponding x, y or z Pauli Matrix and \times corresponds to each of the error locations shown in Fig. 17 (the outer error locations derived from Fig. 4). The internal entries of the fault table correspond to the output probability of detecting a given fault (*column*) by a given test (*row*). A table entry that contains element 0 means that the test corresponding to that element’s row would not detect the fault depicted in that element’s corresponding column. Entries containing p correspond to probabilities of observing given faults (*columns*) under a given input test vector (*row*).

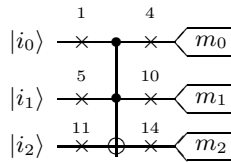


Fig. 17 2–CN gate shown with only the external error locations from Fig. 4.

As mentioned, not all of the error locations shown in Fig. 4 have a corresponding table element in the quantum fault table from Fig. 16. This is due to something known as row and column domination. A dominating row (t_d) has a corresponding entry for each non-zero element in the row being dominated (t_s) and may possibly contain additional non-zero elements ($t_s \subseteq t_d$). Dominating columns are analogous. In the case of the 2–CN gate in Fig. 4 all of the internal error locations {2, 3, 6, 7, 8, 9, 12, 13} were dominated by rows and columns generated by external error locations. A complete test set can therefore be derived considering only the external error locations: {1,4,5,10,11,14} shown in Fig. 17. Each of these error locations may possibly be impacted by three faults (σ_x, σ_y and σ_z) for a total of eighteen table columns. After the introduction of a related Theorem (1) row and column domination will again be discussed.

Theorem 1 provides some insight into the observability of a bit flip error impacting the computational basis. It is based on the following constraints: 1.) *The network is comprised solely of quantum k -CN*

gates, 2.) *The workings of the gates are otherwise nominal.* This theorem states that any σ_x or σ_y fault occurring in a k -CN network is detectable with any computational basis input state. Furthermore, this leads to a relationship between the deterministic presence of a fault in the state vector observed with some probability and the probabilistic presence of a fault observed deterministically (Relating Time and Space Error Models). Theorem 1 is based on the idea that a reversible system preserves information. Moreover, a reversible system preserves the probability that additional information may be present (see Zurek, 1984 [65]). Thus, the probability of detection for fault f observable with \hat{A} for instance, is related only to the probability of f 's presence.

Theorem 1 *Pauli Faults σ_x and σ_y impacting an n qubit network QC comprised of k -CN gates at any gate external error location are trivially detected with any basis state input $|k\rangle$ given an observable in the computational basis.*

Proof Any reversible binary quantum network QC of l qubits and n stages bijectively maps each distinct input $|s\rangle$ to a unique output $|s'\rangle$. Each gate $g \in QC$ is reversible, thus any stage n acting on input vector $|s\rangle$ corresponds to exactly one output vector at the $(n+1)^{th}$ stage. A qubit flip (f_p) occurs before or after any stage n on any wire l , changing the output from the previous stage (and input to the next). Any σ_x or σ_y fault is therefore detectable based on the properties of reversibility [65] with any basis state input $|k\rangle$ given an observable in the computational basis. ■

References [4][6] addressed adapting the rotational and Pauli fault models to quantum test pattern generation; we better explain these findings here. A somewhat obvious corollary of Theorem 1 is the relationship between the probability p that a Pauli fault will occur at some location and the deterministic presence of a rotational fault at some angle θ .²⁵ Consider now a quantum network QC wherein resides error location l perturbed deterministically by a rotational fault f at some angle θ or alternatively by a Pauli fault f at the same location with probability p . One relates p and θ as,

$$\theta = \frac{1}{2} \arcsin(\sqrt{p}). \quad (43)$$

Returning again to Fig. 16. Closer examination reveals that all σ_x and σ_y faults are detected with any basis input vector coinciding with Theorem 1. In the computational basis one can not detect phase faults as they impact the eigenvectors of the computational basis. For a demonstration of this, observe that no basis input vector will detect a σ_z fault. On the other hand, σ_y faults are often detectable with both basis state inputs and superposition inputs, since these faults represent both phase and bit flips. (The column with label σ_{y1} dominates all columns representing σ_z faults: σ_{z1} , σ_{z4} , σ_{z5} , σ_{z10} , σ_{z11} and σ_{z14} .) It should also be mentioned that all σ_z faults (as well as σ_y faults) are detected with input $|+++ \rangle$ and observable \hat{X} and this is true for all quantum switching networks. (The row with entry $|+++ \rangle$ dominates the following rows: $|++- \rangle$, $|+-+ \rangle$, $|+-- \rangle$, $|-++ \rangle$, $|-+- \rangle$, $|--+ \rangle$ and $--- \rangle$.)

Considering again Conjecture 1, aside from row and column domination, the quantum fault table in Fig. 16 illustrates the aforementioned important property of *quantum fault domination*. A test set that is complete for the quantum single fault model (Def. 8) will detect (sample) the accumulated impact of errors at multiple locations. Since quantum noise is defined to be random, a test set that covers all considered faults will sample its uniform distribution. Although on occasion both random and systematic errors may cancel themselves out, we are concerned only with the severity of the accumulated negative impact. This section is concluded by introducing a simple Theorem.

Theorem 2 *All Pauli Faults (σ_x , σ_y and σ_y) impacting an n -qubit quantum switching network are detected with separate applications of any basis input vector $|x\rangle^{\otimes n}$ and superposition state $|+\rangle^{\otimes n}$, where $x \in \{0, 1\}$.*

Proof The Proof follows directly from Theorem 1 and the above discussion of the Fault Table from Fig. 16. ■

5 Conclusion

This work has justified several fault models and discussed the error causing mechanisms that thwart correct function. The fault models that have been justified are: Initialization Errors (Axiom 3, Sec. 3.2), Measurement Faults (Axiom 8, Sec. 3.6), Lost Phase Faults (Axioms 4 and 5, Sec. 3.3), Faded Control

²⁵ Consider for example an optical circuit that applies a partial bit flip at one location based on a mode mismatch [28]. The fault is always present in the state vector, but its observability is probabilistic.

Faults (Axiom 6, Sec. 3.4), and Faded gate faults (Axiom 7, Sec. 3.5). Axioms have been presented that a test set must satisfy in order to drive a quantum network to its bounds of operation for the purpose of error detection. With this justification in place Theorem 1 was presented. The classical test set generation technique known as constructing a fault table, was next adapted to quantum circuits, in Sec. 4. The adapted classical technique, optimizes test plans to detect all of the most common error types. This work therefore considered the prevalent set of errors modeled by unwanted qubit rotations. We found, that isolating a correct circuit from a circuit containing all of the considered Pauli Fault models (given in Axioms 1 & 2) requires applications of just two test vectors as shown in Theorem 2. With the justification of fault models in place, researchers are enabled to develop test plans for quantum circuits with necessary confidence.

Acknowledgments

P.J. Love provided Reference [34] and useful discussions about density matrices and distance measures. Many thanks are also due to J.A. Jones who clearly explained systematic errors and provided references that greatly improved this work. Thanks to D. Maslov for providing comments and useful machine readable quantum circuits [72] and to Quantum Mechanics instructor P. Leung for providing J.D.B. with a very interesting year. J.D.B thanks Jeffrey L. Smith for encouragement and the authors of [16] for useful discussions.

The Quantum Circuit diagrams were drawn in L^AT_EX using Q-circuit [74]. The simulation tool QuIDDPro [73] was used during this study. Portland State University provided student funding, resources, space and support for this project. Support was also given by the Ronald E. McNair Post baccalaureate Achievement Program of Portland State University, and the Korean Advanced Institute of Science and Technology, during parts of this project.

A The Partial Trace

In this Appendix we explain the partial trace [22]. Consider a Hilbert space denoted as A of system $A \otimes B$. We will trace over system A , leaving system B in what is known as a mixed state. We have, $tr_A(|a_1\rangle\langle a_2| \otimes |b_1\rangle\langle b_2|)$. Now consider $|e_i\rangle_i$ as an orthogonal basis for system A , we may write the partial trace as, $\sum_i \langle e_i | a_1 \rangle \langle a_2 | \otimes |b_1\rangle\langle b_2| |e_i\rangle$. After we recall the general fact about tensor products, $|a\rangle\langle b| \otimes |c\rangle\langle d| = |a\rangle\langle c| |b\rangle\langle d|$, it is easy to see a well known equation for the trace of a component part of a composite system, $\sum_i \langle e_i | a_1 \rangle \langle a_2 | |e_i\rangle \otimes |b_1\rangle\langle b_2| = tr(|a_1\rangle\langle a_2|) |b_1\rangle\langle b_2|$.

References

1. W. Kautz, "Automatic fault detection in combinatorial switching networks," Proc. AIEE 2nd Switching Circuit Theory and Logical Design Symp., 1961, pp. 195-214.
2. W.H. Kautz, *Testing faults in combinational cellular logic arrays*, Proceedings of 8th annu. Symp. Switching and Automata Theory, 1971, pp. 161-174.
3. S.K. Shukla, R. Kam, S.C. Goldstein, F. Brewer, K. Banejee and S. Basu, "Nano, Quantum, and Molecular Computing: Are we Ready for the Validation and Test Challenges?," IEEE Pannel Discussion, 0-7803-8236-6, 2003, pp. 3-7, online: <http://www.ece.ucsb.edu/>.
4. J.D. Biamonte and M.A. Perkowski, "Testing a Quantum Computer," Proceedings of, KIAS-KAIST 5th Workshop on Quantum Information Science, Seoul Korea, August 29th-31st, 2004, pp. 16.
5. J.P. Hayes, I. Polian and B. Becker, "Testing for Missing-Gate Faults in Reversible Circuits," Proc. Asian Test Symposium, Taiwan, 2004, pages 6.
6. M.A. Perkowski et al., "Test Generation and Fault Localization for Quantum Circuits," Proc 35th ISMVL, May 2005, pp. 62-68, DOI: 10.1109/ISMVL.2005.46.
7. K.N. Patel, J.P. Hayes and I.L. Markov, "Fault Testing for Reversible Circuits," IEEE Trans. on CAD, 23(8), 2004, pp. 1220-1230, [quant-ph/0404003](http://dx.doi.org/10.1109/9804003).
8. D. Deutsch, "Quantum computational networks," Proceedings of the Royal Society of London. Series A, Mathematical and Physical Sciences, Volume 425, Issue 1868, 1989, pp. 73-90.
9. M.H.S. Amin, M. Grajcar, E. Il'ichev', A.M. Maassen van den Brink, G. Rose, A.Y. Smirnov and A.M. Zagorskin. "Superconducting Quantum Storage and Processing," IEEE Interational Solid-State Circuits Conference, ISSCC, Session 16, 2004, 10 pages.
10. J. Jones, M. Mosca and R. Hansen, "Implementation of a Quantum Search Algorithm on a Nuclear Magnetic Resonance Quantum Computer," Nature Vol. 393, 1998, pp. 344-346, [quant-ph/9805069](http://dx.doi.org/10.1038/9805069).
11. J. Jones and M. Mosca, "Approximate quantum counting on an NMR ensemble quantum computer," Phys.Rev.Lett. 83:1050, 1999, 4 pages, [quant-ph/9808056](http://dx.doi.org/10.1103/PhysRevLett.83.1050).

12. A.M. Steane and D.M. Lucas, "Quantum computing with trapped ions, atoms and light," Fortschritte der Physik, special issue, 2000, 17 pages, [quant-ph/0004053](#).
13. A.M. Childs, I.L. Chuang and D.W. Leung, "Realization of quantum process tomography in NMR," Phys. Rev. A Iss. 64, 012314, 2001, 8 pages, [quant-ph/0012032](#).
14. I.L. Chuang and M.A. Nielsen, "Prescription for experimental determination of the dynamics of a quantum black box," J. Mod. Opt. 44, 2455, 1997, 6 pages, [quant-ph/9610001](#).
15. G.M. D'Ariano and P. Lo Presti, "Measuring Experimentally the Matrix Elements of an Arbitrary Quantum Operation," Phys. Rev. Lett. Vol. 86, 2001, 41954198, DOI: 10.1103/PhysRevLett.86.4195.
16. K. Kim, M. Song, S. Lee, and J-S. Lee, "Quantum Process Tomography with Arbitrary Number of Ancillary Qubits in Nuclear Magnetic Resonance," In Pres, Journal of Korean Physical Society (JKPS), 2005, 8 pages.
17. J.B. Altepeter, D. Branning, E. Jeffrey, T.C. Wei, P.G. Kwiat, R.T. Thew, J.L. O'Brien, M.A. Nielsen and A.G. White, "Ancilla-assisted quantum process tomography," Phys. Rev. Lett. 90, 193601, 2003, 4 pages, [quant-ph/0303038](#).
18. P.W. Shor, "Polynomial-Time Algorithms for Prime Factorization and Discrete Logarithms on a Quantum Computer," Proceedings of the 35th Annual Symposium on Foundations of Computer Science, Santa Fe, NM, Nov. 20-22, 1994, pp 124-134 [quant-ph/9508027](#).
19. U. Kalay, M.A. Perkowski and D.V. Hall "A Minimal Universal Test Set for Self-Test of EXOR-Sum-of-Product Circuits," IEEE Transactions on Computers, vol. 49 no. 3, 2000, pp. 267-276.
20. L.K. Grover, "Quantum mechanics helps in searching for a needle in a haystack," Physical Review Letters Iss. 2, 79:325, 1997, pp. 325-328 [quant-ph/9706033](#).
21. J.S. Allen, J.D. Biamonte and M.A. Perkowski, "ATPG for Reversible Circuits using Technology-Related Fault Models," To appear, Proc. 7th International Symposium on Representations and Methodology of Future Computing Technologies, RM2005, Tokyo, Japan, September 5th and 6th, 2005, 8 pages.
22. M.A. Nielsen and I.L. Chuang, "Quantum Computation and Quantum Information," Cambridge Univ. Press, 2000.
23. M. Oskin, "Quantum Computing Lecture Notes," Class Notes, University of Washington, 2004, [cs.washington.edu](#).
24. D. Deutsch, "Video Lectures on Quantum Computation," 2004, free online, [www.quiprocone.org](#).
25. A.W. Harrow and M.A. Nielsen, "How robust is a quantum gate in the presence of noise?," Phys. Rev. A Vol. 68, 012308, 2003, 14 pages, [quant-ph/0301108](#).
26. M. Mosca, "Quantum Computer Algorithms," PhD thesis, University of Oxford, 1999, <http://www.cacr.math.uwaterloo.ca/>.
27. A. Barenco, C.H. Bennett, R. Cleve, D.P. DiVincenzo, N. Margolus, P.W. Shor. T. Sleator, J. Smolin, and H. Weinfurter, "Elementary gates of quantum computation," Phys.Rev.A, Vol. 52(5):3457-3467, 1995, 31 pages, [quant-ph/9503016](#).
28. J.L. O'Brien, G.J. Pryde, A. Gilchrist, D.F.V. James, N.K. Langford, T. C. Ralph and A. G. White, "Quantum process tomography of a controlled-NOT gate," Phys. Rev. Lett. Vol. 93, 080502, 2004, 4 pages, [quant-ph/0402166](#).
29. M.A. Nielsen, "Quantum information theory," PhD thesis, University of New Mexico, Report UNM-98-08 1998, 259 pages, [quant-ph/0011036](#).
30. D.W. Leung, "Towards Robust Quantum Computation," PhD thesis, Stanford University, 2000, 243 pages, [cs/0012017](#).
31. D.F.V. James, P.G. Kwiat, W.J. Munro and A.G. White, "On the Measurement of Qubits," Phys. Rev. A Vol. 64, 052312, 2001, 23 pages, [quant-ph/0103121](#).
32. M.A. Nielsen, "A simple formula for the average gate fidelity of a quantum dynamical operation," Phys. Lett. A Vol. 303 4 , 2002, pp. 249-252, [quant-ph/0205035](#).
33. J.L. Dodd and M.A. Nielsen, "A simple operational interpretation of the fidelity," Phys. Rev. A Vol. 66, 044301, 2002, 1 page, [quant-ph/0111053](#).
34. A. Gilchrist, N.K. Langford and M.A. Nielsen, "Distance measures to compare real and ideal quantum processes," Phys. Rev. A Vol. 71, 062310, 2005, 14 pages, [quant-ph/0408063](#).
35. M.D. Bowdrey and J.A. Jones, "A Simple and Convenient Measure of NMR Rotor Fidelity," JAJ-QP-01-01, 2001, 2 pages [quant-ph/0103060](#).
36. M.D. Bowdrey, D.K.L. Oi, A.J. Short, K. Banaszek and J.A. Jones, "Fidelity of Single Qubit Maps," Phys. Lett. A Vol. 294, 258, 2002, 5 pages, (Supersedes [quant-ph/0103090](#) and [quant-ph/0103060](#)), (2002), [quant-ph/0201106](#).
37. M. Steffen, L.M.K. Vandersypen and I.L. Chuang. "Toward Quantum Computation: A Five-Qubit Quantum Processor," IEEE Micro, 2001, pp. 24-34, DOI: 10.1109/40.918000.
38. A.G. White, A. Gilchrist, G.J. Pryde, J.L. O'Brien, M.J. Bremner and N.K. Langford, "Measuring Controlled-NOT and two-qubit gate operation," , 2003, 10 pages, [quant-ph/0308115](#).
39. J.A. Jones, "NMR Quantum Computing," in Quantum Computation and Quantum Information Theory, World Scientific, Singapore 2001, <http://nmr.physics.ox.ac.uk>;
40. "Nuclear Magnetic Resonance Quantum Computation," in Quantum Entanglement and Information Processing, D. Esteve, J.-M. Raimond, and J. Dalibard (Eds.), Elsevier Science, 2004, <http://nmr.physics.ox.ac.uk>.
41. J.A. Jones and M. Mosca, "Implementation of a Quantum Algorithm to Solve Deutsch's Problem on a Nuclear Magnetic Resonance Quantum Computer," Journal of Chemical Physics Vol. 109, August 1st 1998, pp. 1648-1653, [quant-ph/9801027](#).
42. L.M.K. Vandersypen, M. Steffen, G. Breyta, C.S. Yannoni, M.H. Sherwood and I.L. Chuang, "Experimental realization of Shor's quantum factoring algorithm using nuclear magnetic resonance," Nature Vol. 414, 2001, pp. 883-887, [quant-ph/0112176](#).

43. J.L. O'Brien, G.J. Pryde, A.G. White, T.C. Ralph and D. Branning, "*Demonstration of an all-optical quantum controlled-NOT gate*," Nature Vol. 426, 2003, 5 pages, [quant-ph/0403062](#).
44. P.W. Shor, "*Fault-Tolerant Quantum Computation*," 37th Symposium on Foundations of Computing, IEEE Computer Society Press Vol. 37, 1996, pp. 56-65, [quant-ph/9605011](#).
45. E. Knill, R. Laflamme and W.H. Zurek, "*Resilient Quantum Computation: Error Models and Thresholds*," Proc. Mathematical, Physical Engineering Sciences Vol. 454, 1997, pp. 365-384 [quant-ph/9702058](#).
46. C.H. Bennett, D.P. DiVincenzo, J.A. Smolin, W.K. Wootters, "*Mixed State Entanglement and Quantum Error Correction*," Phys.Rev. A Vol. 54, 1996, pp. 3824-3851, [quant-ph/9604024](#).
47. L.M.K. Vandersypen, C.S. Yannoni, and I.L. Chuang, "*Liquid State NMR Quantum Computing*," Encyclopedia of Nuclear Magnetic Resonance Vol. 9: Advances in NMR, 2002, pp. 687697, <http://qt.tn.tudelft.nl>.
48. P.J. Love and B. Boghosian, "*From Dirac to Diffusion: Decoherence in Quantum Lattice Gases*," To appear in QIP, 2005, [quant-ph/0507022](#).
49. E. Knill, R. Laflamme, A. Ashikhmin, H. Barnum, L. Viola and W.H. Zurek. "*Introduction to Quantum Error Correction*," LA Science Vol. 27, 2002, 22 pages, [quant-ph/0207170](#).
50. D. Aharonov and M. Ben-Or, "*Fault-Tolerant Quantum Computation With Constant Error Rate*," Proc. 29th Ann. ACM Symp. on Theory of Computing, New York, 1998, p. 176, [quant-ph/9611025](#); [quant-ph/9906129](#).
51. S. Bettelli, "*Quantitative model for the effective decoherence of a quantum computer with imperfect unitary operations*," Physical Review A Vol. 69, 042310, 2004, 14 pages, [quant-ph/0310152](#).
52. A. Barenco, T.A. Brun, R. Schack, and T.P. Spiller, "*Effects of noise on quantum error correction algorithms*," Modern Physics Letters A Vol. 13, 1998, pp. 2503-2512, [quant-ph/9612047](#).
53. N. Shenvi, K.R. Brown and K.B. Whaley, "*Effects of Random Noisy Oracle on Search Algorithm Complexity*," Phys. Rev. A Vol. 68, 052313, 2003, 11 pages [quant-ph/0304138](#).
54. S. Kak, "*The Initialization Problem in Quantum Computing*," Foundations of Physics, vol 29, 1999, pp. 267-279, [quant-ph/9805002](#).
55. M.S. Anwar, D. Bazina, H. Carteret, S.B. Duckett, T.K. Halstead, J.A. Jones, C.M. Kozak and R.J.K. Taylor, "*Preparing High Purity Initial States for Nuclear Magnetic Resonance Quantum Computing*," Phys. Rev. Lett. Vol. 93, 040501, 2004, 3 pages, [quant-ph/0312014](#).
56. A.M. Childs, J. Perskill and J. Renes, "*Quantum information and precision measurement*," J.Mod.Opt. Vol. 47, pp. 155-176, 2000, [quant-ph/9904021](#).
57. C.P. Williams and S.H. Clearwater, "*Explorations in quantum computing*," Springer Verlag, 1998.
58. H.K. Cummins and J.A. Jones, "*Use of composite rotations to correct systematic errors in NMR quantum computation*," New Journal of Physics, Vol 2 6.1-6.12, 2000, 11 pages, [quant-ph/9911072](#).
59. S. Lee, J.S. Lee, T. Kim, J.D. Biamonte and M.A. Perkowski, "*The Cost of Quantum Gate Primitives*," In Pres., Journal of Multiple-Valued Logic and Soft Computing, 2005, 10 pages.
60. G.J. Ni, and S.Q. Chen, "*Advanced Quantum Mechanics*," Rinton Press Inc, 2002, 465 pp..
61. H.K. Cummins, G. Llewellyn, and J.A. Jones, "*Tackling Systematic Errors in Quantum Logic Gates with Composite Rotation*," Phys. Rev. A Vol. 67, 042308, 2003, 7 pages, [quant-ph/0208092](#).
62. J.A. Jones, *Conversation at Clarendon Laboratory*.
63. K.M. Obenland and A.M. Despain, "*Impact of Errors on a Quantum Computer Architecture*," Technical Report, Information Sciences Institute, University of Southern California, Oct 1st, 1996, <http://www.isi.edu/>.
64. J.A. Jones and E. Knill, "*Efficient Refocussing of One Spin and Two Spin Interactions for NMR Quantum Computation*," J.Magn.Resonance Vol. 141 , pp. 322-325, 1999, [quant-ph/9905008](#).
65. W.H. Zurek, "*Reversibility and Stability of Information Processing Systems*," Phys. Rev. Lett. Vol. 53, 1984, pp. 391-394, DOI: 10.1103/PhysRevLett.53.391.
66. L.K. Grover, "*A different kind of quantum search*," 13 pages, 2005, [quant-ph/0503205](#).
67. L. Xiao and J.A. Jones, "*Error tolerance in an NMR Implementation of Grover's Fixed-Point Quantum Search Algorithm*," in press Phys.Rev.A, 2005, 5 pages, [quant-ph/0504054](#).
68. B.W. Reichardt and L.K. Grover, "*Quantum error correction of systematic errors using a quantum search framework*," free online, 2005, 6 pages, [quant-ph/0506242](#).
69. J.A. Jones, R.H. Hansen and M. Mosca, "*Quantum Logic Gates and Nuclear Magnetic Resonance Pulse Sequences*," J.Magn.Resonance Vol. 135, 1998, pp. 353-360, [quant-ph/9805070](#)
70. P.P. Rohde, G.J. Pryde, J.L. O'Brien and T.C. Ralph, "*Quantum gate characterization in an extended Hilbert space*," free online, 2004, 4 pages, [quant-ph/0411144](#).
71. E. J. McCluskey and C.W. Tseng, "*Stuck-fault tests vs. actual defects*," in Proc. 2000 Int. Test Conf., Atlantic City, 2000, pp. 336343.
72. D. Maslov, C. Young, D. M. Miller and G. W. Dueck, "*Quantum Circuit Simplification Using Templates*," In Proc. DATE Conference, Munich, Germany, March 2005, pp. 1208-1213.
73. G. F. Viamontes, I. L. Markov, J. P. Hayes, "*Graph-based simulation of quantum computation in the density matrix representation*," Quantum Information and Computation, Vol. 5, No. 2, 2005, pp. 113-130.
74. B. Eastin and S.T. Flammia, "*Q-circuit Tutorial*," free online, 2004, 7 pages, [quant-ph/0406003](#).